

ORIGINAL ARTICLE

Optimization of nonlinear quarter car suspension–seat–driver model



Mahesh P. Nagarkar^{a,b,*}, Gahininath J. Vikhe Patil^c, Rahul N. Zaware Patil^d

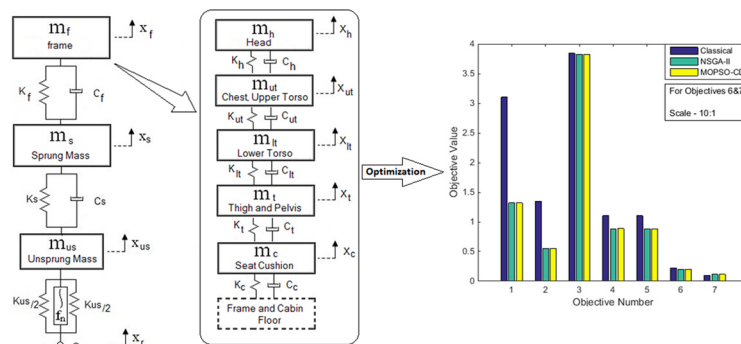
^a SCSM College of Engineering, Ahmednagar 414005, MS, India

^b Research Department of Mechanical Engineering, AVCoE, Sangamner 422605, MS, India

^c AVCoE, Sangamner 422605, Dist – Ahmednagar, MS, India

^d PDVVP CoE, Vilad Ghat, Ahmednagar 414111, MS, India

GRAPHICAL ABSTRACT



ARTICLE INFO

Article history:

Received 10 February 2016

Received in revised form 25 April 2016

Accepted 26 April 2016

Available online 4 May 2016

ABSTRACT

In this paper a nonlinear quarter car suspension–seat–driver model was implemented for optimum design. A nonlinear quarter car model comprising of quadratic tyre stiffness and cubic stiffness in suspension spring, frame, and seat cushion with 4 degrees of freedom (DoF) driver model was presented for optimization and analysis. Suspension system was aimed to optimize the comfort and health criterion comprising of Vibration Dose Value (VDV) at head, frequency weighted RMS head acceleration, crest factor, amplitude ratio of head RMS acceleration to seat RMS accelera-

* Corresponding author. Tel.: +91 241 2568383; fax: +91 241 2568384.

E-mail address: maheshnagarkar@rediffmail.com (M.P. Nagarkar).

Peer review under responsibility of Cairo University.



Production and hosting by Elsevier

<http://dx.doi.org/10.1016/j.jare.2016.04.003>

2090-1232 © 2016 Production and hosting by Elsevier B.V. on behalf of Cairo University.

This is an open access article under the CC BY-NC-ND license (<http://creativecommons.org/licenses/by-nc-nd/4.0/>).

Nomenclature

A	system matrix	k_{snl}	nonlinear spring stiffness (N/m ³)
AR_{h}	amplitude ratio of head RMS acceleration to seat RMS acceleration	k_{t}	tyre stiffness (N/m)
AR_{ut}	amplitude ratio of upper torso RMS acceleration to seat RMS acceleration	k_{tnl}	nonlinear tyre stiffness (N/m ²)
A_{wh}	frequency weighted RMS head acceleration (m/s ²)	m	mass (kg)
$A_{\text{w_spr}}$	frequency weighted RMS sprung mass acceleration (m/s ²)	VDV_{h}	vibration dose value at head (m/s ^{1.75})
a_{wh}	frequency weighted head acceleration (m/s ²)	x_{r}	road profile (m)
c	damping coefficient (N s/m)	x, \dot{x}, \ddot{x}	displacement (m), velocity (m/s) and acceleration (m/s ²)
c_{lt}	lumber spine damping (N s/m)	<i>Subscripts (unless and otherwise stated)</i>	
c_{ut}	thoracic spine damping (Ns/m)	s	sprung
c_{h}	cervical spine damping (N s/m)	us	unsprung
f_{obj}	objective function	f	frame
k	stiffness (N/m)	c	seat cushion
k_{lt}	lumber spine stiffness (N/m)	tp	thigh and pelvis
k_{ut}	thoracic spine stiffness (N/m)	lt	lower torso
k_{h}	cervical spine stiffness (N/m)	ut	upper torso
		h	head

Keywords:

Nonlinear quarter car
Genetic algorithm
Multi-objective optimization
MOSPO-CD
Quadratic tyre stiffness
Cubic stiffness in suspension spring

tion and amplitude ratio of upper torso RMS acceleration to seat RMS acceleration along with stability criterion comprising of suspension space deflection and dynamic tyre force. ISO 2631-1 standard was adopted to assess ride and health criterions. Suspension spring stiffness and damping and seat cushion stiffness and damping are the design variables. Non-dominated Sort Genetic Algorithm (NSGA-II) and Multi-Objective Particle Swarm Optimization – Crowding Distance (MOPSO-CD) algorithm are implemented for optimization. Simulation result shows that optimum design improves ride comfort and health criterion over classical design variables.

© 2016 Production and hosting by Elsevier B.V. on behalf of Cairo University. This is an open access article under the CC BY-NC-ND license (<http://creativecommons.org/licenses/by-nc-nd/4.0/>).

Introduction

Suspension system along with seat has been widely used in vehicles to isolate passengers from shock and vibrations arising due to road unevenness. Seat-suspension system thus provides ride comfort, reduces fatigue during driving conditions and improves health and safety of drivers. Other performance requirements for a suspension system are to adequately support the vehicle weight, to maintain the wheels in the appropriate position so as to have a better handling and to keep the tyre in contact with the ground. The passive suspension systems are the trade-off between ride comfort and handling [1]. Due to the conflicting requirements, the suspension system has been investigated by many researchers to find the optimal trade-off amongst the conflicting requirements.

Gobbi and Mastinu [2] presented Multi-Objective Programming and Monotonicity analysis based optimization method for finding the trade-off for conflicting performance requirements such as discomfort, road holding and working space. A 2 DoF quarter car model running on random road profile was used. The optimal settings of the vehicle suspension parameters such as tyre stiffness, spring stiffness, and damping were derived either symbolically and/or numerically. Verros and Natsiavas [3] presented optimization of suspension stiffness and damping. A quarter car model travelling on a random road profile was used for optimization study. Authors had used and presented a critical comparison of quarter car models

with passive linear and dual-rate suspension dampers and semi-active sky-hook damping models. Optimization of a light commercial vehicle to improve vehicle ride and handling was performed by Özcan et al. [4] using a quarter car and the half car models in Matlab/Simulink® environment. The performance criterions considered were RMS body acceleration, tyre forces, and body roll. The performance of the optimized suspension unit was verified using Carmaker model.

Molina-Cristobal et al. [5] had presented multi-objective optimization of a passive suspension system using quarter car model using meta-heuristic optimization with the multi-objective genetic algorithm (MOGA) and bilinear matrix inequalities (BMI) techniques. Ride comfort using RMS body vertical acceleration and road holding criterions were used as objective functions during optimization. Chi et al. [6] had presented optimization of linear quarter car model using three different techniques namely genetic algorithm (GA), pattern search algorithm (PSA) and sequential quadratic program (SQP) subjected to body acceleration, suspension working space, and dynamic tyre load as design criterions. Gomes [7] presented optimization of 2-DoF quarter car model travelling over a random road surface. The particle swarm optimization (PSO) algorithm is used for optimization. Minimization of dynamic vehicle load and minimization of suspension deflection were used as objective functions in two optimization examples. Baumal et al. [8] presented GA-based optimization of half car model with an objective to minimize acceleration

of the passenger’s seat, subject to constraints such as road holding and suspension working space.

Aforesaid literature had studied suspension system as the most significant factor and optimized the suspension parameters, spring stiffness and damping, for ride comfort, suspension space, road holding, and dynamic tyre force as objective functions.

Kuznetsov et al. [9] had presented optimization of quarter car model coupled with a driver. A 3-DoF driver–car model, a quarter car having 2 DoF and a driver having 1 DoF, is developed for optimization. Ride comfort criteria as per ISO 2631-1 were used for optimization using the algorithm for global optimization problems (AGOP). Gundogdu [10] presented optimization of quarter car suspension system with seat using GA. A two DoF linear quarter car model was developed including 2-DoF lumped mass driver model. Objective function is formulated using head acceleration, crest factor, suspension deflection and tyre deflection objective functions. Objective functions are converted into uni-objective function using non-dimensional expressions, giving equal importance to each of the objective functions. Badran et al. [11] presented optimization of a human-car suspension system using GA. Quarter car model is used as a vehicle model. Seat acceleration, head acceleration, and suspension working space were used as the optimization criterion. The objective function was converted into an uni-objective function using weighting parameters. Results are compared to step and sinusoidal road profile. Thus, it is observed that a quarter car suspension system along with driver model was optimized using uni-objective function although the optimization problem is of multi-objective nature [10,11]. Also, the human bio-mechanical model considered for the study is either 1 DoF [9] or 2 DoF [10].

Patil and Palanichamy [12] showed that body parts such as head, torso, and pelvis respond to a much greater extent to road induced vibrations as compared to seat response. Hence, car suspension system should be aimed to optimize considering responses of other body parts such as head, torso, thorax, abdomen, and diaphragm. This study presents the multi-objective optimization of nonlinear quarter car model coupled with a 4-DoF driver model. A nonlinear quarter car model having quadratic tyre stiffness and cubic stiffness in suspension spring is modelled. Multi-objective optimization is presented using two optimization algorithms – Non-dominated Sort Genetic Algorithm II (NSGA-II) and Multi-Objective Particle Swarm Optimization with Crowding Distance (MOPSO-CD). Vibration Dose Value (VDV) at head, Frequency weighted Root Mean Square (hereafter called as RMS) head acceleration, amplitude ratio of head RMS acceleration to seat RMS acceleration, amplitude ratio of upper torso RMS acceleration to seat RMS acceleration, crest factor, suspension space deflection and dynamic tyre force in terms of dynamic tyre deflection are considered as objective functions for optimization. Results are presented in tabular as well as graphical format.

Methodology

Mathematical modelling – nonlinear quarter car suspension–seat–driver model

To study the behaviour of a dynamic system and to optimize the same, mathematical model of the system is required.

Modelling of a suspension system is done in the vertical plane. Longitudinal or transverse deflections of the suspension components are considered negligible in comparison with vertical deflections. The model is simple, yet consists of basic elements of the suspension system such as sprung mass m_s (representing chassis) and unsprung mass m_{us} (representing wheel assembly and axle). Springs and dampers, representing suspension element, are connected between the sprung and unsprung masses and spring, representing tyre, is connected between unsprung mass and ground respectively.

A suspension system of commercial vehicles generally consists of coil springs. During the mathematical modelling of a suspension system, the elements of a suspension system, springs and dampers, are considered as linear. But the spring exhibits nonlinear nature. Also, the stiffness of pneumatic tyre is nonlinear in nature. Hence, while mathematical modelling of a suspension system these nonlinear elements should be considered. McGee et al. [13] presented a detailed study on nonlinearities in the suspension system. Frequency domain technique for characterizing the nonlinearities is presented and validated by laboratory shaker with road data for validation. It was concluded that suspension system has quadratic and cubic stiffness nonlinearities and Coulomb friction. Zhu and Ishitobi [14] presented chaotic response of 7 DoF model subjected to nonlinear tyre stiffness and nonlinear suspension spring stiffness. Lixia and Wanxiang [15] presented bifurcation and chaotic response of 2 DoF vehicle model having nonlinearities in tyre stiffness and suspension spring stiffness.

In the present analysis, a nonlinear quarter car model having quadratic tyre stiffness and cubic stiffness in suspension spring as nonlinearities is considered along with seat suspension model consisting of a frame and cushion is shown in Fig. 1a.

Human body is very complex and sophisticated dynamic system. In the literature, many mechanical models have been developed based on lumped-parameter models. Coermann [16] developed 1-DoF model consisting of single second order differential equation. Wei and Griffin [17] developed 1 and 2 DoF linear models with an assumption that human body is

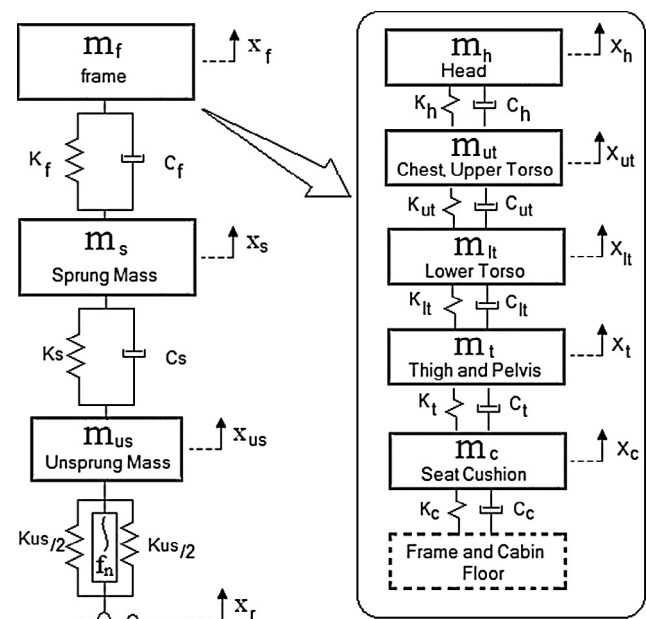


Fig. 1a Quarter car–seat–suspension – human model.

seated firmly on the seat. In the early studies, 3 DoF seated human subject was modelled by Suggs et al. [18] as damped spring-mass model. Wan and Schimmels [19] and Boileau and Rakheja [20] modelled a 4 DoF lumped parameter model.

In this study a 4 DoF lumped parameter human model suggested by Boileau and Rakheja [20] was used in optimization study. It consists of head and neck mass (m_h), chest and upper torso mass (m_{ut}), lower torso mass (m_{lt}) and thigh and pelvis mass (m_t). A 4-DoF human bio-mechanical model developed by Boileau and Rakheja [20] considers typical driving conditions such as seated posture with feet support and hands held in driving conditions. During model development, magnitude and phase characteristics of driving point mechanical impedance (DPMI) and seat-to-head transmissibility (STHT) are satisfied. As DPMI signifies the dynamic load at the point of input whereas STHT signifies dynamic behaviour of body parts, DPMI of seated subjects was determined from laboratory experiments whereas STHT values are determined from published data. To analyse whole body vibrations, the bio-dynamic human model parameters are estimated by simultaneously optimizing the magnitude and phase responses of DPMI and STHT, under driving conditions [20].

Arslan [21] conducted experimental study on three different bio-dynamic models subjected to three different road types to provide quantified assessment. To assess the bio-dynamic models, experimental data on seated subject are recorded and compared with simulated data of models. Assessment of models is based on root mean square difference (RMSD) and Pearson correlation coefficient (PCC) between simulated and experimental results. According to results, the model suggested by Boileau and Rakheja [20] showed the best correlation with experimental data.

According to D'Alembert's principle, the governing equations of motion representing nonlinear quarter car suspension-seat-human model are:

$$\left. \begin{aligned} m_{us}\ddot{x}_{us} &= -k_t(x_{us} - x_r) + k_s(x_s - x_{us}) + c_s(\dot{x}_s - \dot{x}_{us}) + k_{tnl}(x_{us} - x_r)^2 + k_{snl}(x_s - x_{us})^3 \\ m_s\ddot{x}_s &= -k_s(x_s - x_{us}) - c_s(\dot{x}_s - \dot{x}_{us}) - k_{snl}(x_s - x_{us})^3 + k_f(x_f - x_s) + c_f(\dot{x}_f - \dot{x}_s) \\ m_f\ddot{x}_f &= -k_f(x_f - x_s) - c_f(\dot{x}_f - \dot{x}_s) + k_c(x_c - x_f) + c_c(\dot{x}_c - \dot{x}_f) \\ m_c\ddot{x}_c &= -k_c(x_c - x_f) - c_c(\dot{x}_c - \dot{x}_f) + k_{tp}(x_t - x_c) + c_{tp}(\dot{x}_t - \dot{x}_c) \\ m_t\ddot{x}_t &= -k_{tp}(x_t - x_c) - c_{tp}(\dot{x}_t - \dot{x}_c) + k_{lt}(x_{lt} - x_t) + c_{lt}(\dot{x}_{lt} - \dot{x}_t) \\ m_{lt}\ddot{x}_{lt} &= -k_{lt}(x_{lt} - x_t) - c_{lt}(\dot{x}_{lt} - \dot{x}_t) + k_{ut}(x_{ut} - x_{lt}) + c_{ut}(\dot{x}_{ut} - \dot{x}_{lt}) \\ m_{ut}\ddot{x}_{ut} &= -k_{ut}(x_{ut} - x_{lt}) - c_{ut}(\dot{x}_{ut} - \dot{x}_{lt}) + k_h(x_h - x_{ut}) + c_h(\dot{x}_h - \dot{x}_{ut}) \\ m_h\ddot{x}_h &= -k_h(x_h - x_{ut}) - c_h(\dot{x}_h - \dot{x}_{ut}) \end{aligned} \right\} \quad (1)$$

The nonlinear quarter car seat-suspension-driver model parameters are as follows:

$$\begin{aligned} m_h &= 5.31; & c_h &= 400; & k_h &= 310,000; \\ m_{ut} &= 28.49; & c_{ut} &= 4750; & k_h &= 183,000; \\ m_{lt} &= 8.62; & c_{lt} &= 4585; & k_{lt} &= 162,800; \\ m_t &= 12.78; & c_t &= 2064; & k_t &= 90,000; \\ m_c &= 1; & c_c &= 200; & k_c &= 18,000; \\ m_f &= 15; & c_f &= 830; & k_f &= 31,000; \\ m_s &= 290; & c_s &= 700; & k_s &= 23,500; & k_{snl} &= 100k_s [15]; \\ m_{us} &= 40; & k_t &= 190,000; & k_{tnl} &= 1.5 k_t [14]. \end{aligned}$$

The nonlinear and linear quarter car-seat-suspension model along with human model is simulated in Matlab/Simulink®. A nonlinear quarter car model, having quadratic tyre stiffness nonlinearity in tyre and cubic stiffness in suspension spring, and linear quarter car model are modelled and simulated. During simulation of linear quarter car model, nonlinear parameters such as k_{tnl} and k_{snl} , are kept zero. Both models are simulated using input as step (step size of 0.1 unit), bump (bump height of 0.1 unit) and class C road.

From step response, it is observed that VDV at head and RMS head acceleration of nonlinear model is $5.8180 \text{ m/s}^{1.75}$ and 1.5636 m/s^2 respectively whereas for linear model it is $3.7402 \text{ m/s}^{1.75}$ and 1.0369 m/s^2 . The VDV at head and RMS head acceleration of the nonlinear system is greater than linear system due nonlinearities present in tyre and suspension spring. Maximum head acceleration of a nonlinear system is higher than the linear system. The increase in head acceleration of nonlinear system than that of the linear system can also be observed in frequency response plots. The crest factor, amplitude ratio AR_h and AR_ut are higher for a nonlinear model as compared to the linear model. As AR_h and AR_ut ratios are higher for a nonlinear system hence more magnitude of accelerations will be transferred from the seat. RMS Sprung mass acceleration of a nonlinear system is also higher than the linear system due to quadratic nonlinearity in tyre and cubic nonlinearity in suspension spring. Refer Fig. 1b and Table 1.

Fig. 1b also represents frequency response of linear and nonlinear quarter car with a human model. For linear and nonlinear models, the first peak at head acceleration is observed at 3 Hz whereas the second peak at wheel hop occurs at 10 Hz. For upper torso frequency response, the first peak is observed at upper torso acceleration at 3 Hz and the second peak is observed at wheel hop at 10 Hz for both linear and nonlinear models. The frequency response of sprung mass acceleration shows the first peak at sprung mass acceleration

at 3 Hz for both linear and nonlinear models whereas the second peak at wheel hop is observed at 10 Hz for the linear system and 14 Hz at the nonlinear system. This is due to quadratic nonlinearity in tyre and cubic nonlinearity in suspension spring.

From frequency response plots, shown in Fig. 1b, it is observed that the magnitude of head acceleration gain, upper torso acceleration gain and sprung mass acceleration gain of nonlinear system is greater than that of linear system. This indicates more acceleration transmission in nonlinear system due to nonlinearities. This is also evident from the time

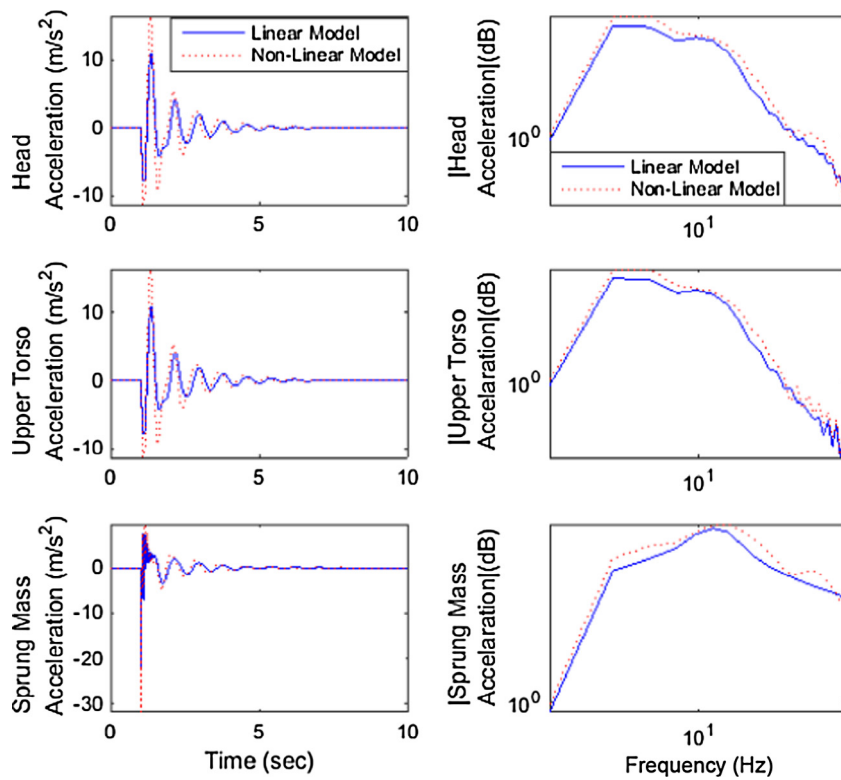


Fig. 1b Step input – linear and nonlinear quarter model – time and frequency response.

Table 1 Comparative analysis of linear and nonlinear model.

	Step input		Bump input		Class C road input	
	Linear	Non linear	Linear	Non linear	Linear	Non linear
VDV	3.7402	5.8180	1.5784	1.6639	3.6110	5.4373
A_{wh}	1.0369	1.5636	0.7023	0.7350	1.0737	1.5685
Max a_{wh}	10.8769	16.4397	2.7950	2.9612	14.8633	18.9152
CF	10.4901	10.5141	3.9024	3.9468	11.5218	12.0593
AR_h	1.1225	1.1487	1.1255	1.1276	1.1133	1.1273
AR_ut	1.1199	1.1457	1.1206	1.1229	1.1113	1.1250
A_{w_spr}	1.2668	1.6464	2.0467	2.0672	0.5247	0.7470

responses of nonlinear system. Refer Fig. 1b. Similar trends are observed for bump response. Refer Fig. 1c for time and frequency responses and Table 1 for results.

McGee et al. [13] already presented a detailed study on frequency domain using laboratory shaker data. Hence for class C road input, only time domain results are shown in Fig. 1d. It is observed that RMS head acceleration, VDV at head, upper torso acceleration, and sprung mass acceleration are on the higher side for a nonlinear model as compared to the linear model. Also CF, AR_h and AR_ut are greater for the nonlinear system as compared to the linear system. Hence, nonlinearities should be adequately addressed during the ride, control and optimization applications of vehicle models.

Multi-objective optimization

Researchers have invented several meta-heuristic optimization algorithms to optimize the problems in several fields. These algorithms have implemented on several mathematical prob-

lems involving single objective optimization to multi-objective optimization and provided excellent results.

The suspension system has to perform several conflicting objectives such as ride comfort, road holding, and suspension/rattle space requirements. Also, in this study, human model is incorporated to optimize the objective functions considering the human body responses rather than only the seat. Thus, the optimization problem becomes multi-objective in nature (consisting of Head VDV, RMS head acceleration, crest factor, AR_h, AR_ut, suspension space requirement and dynamic tyre force/deflection as objective functions) with conflicts. As compared to a single objective optimization problem, a multi-objective optimization (MOO) problem has to satisfy several objectives simultaneously. Hence, multi-objective optimization using genetic algorithm (GA) and particle swarm optimization (PSO) algorithms are implemented to solve the optimization problem.

In the solution of MOO problems, MOO forms a Pareto optimal front consisting of multiple optimal solutions. Genetic

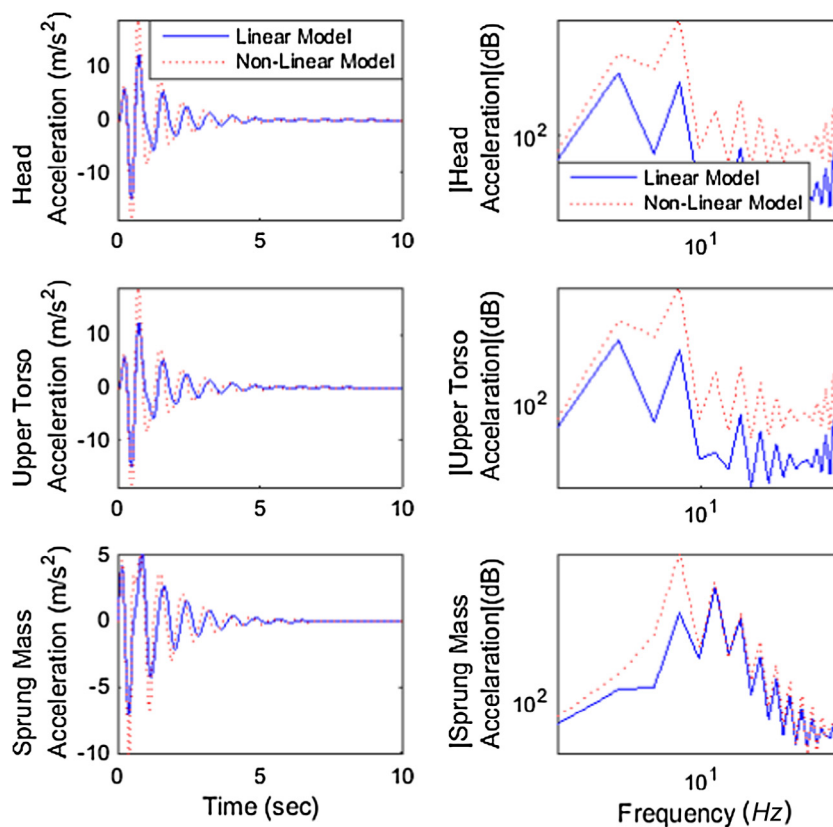


Fig. 1c Bump input – linear and nonlinear quarter model – time and frequency response.

Algorithm (GA) is implemented to optimize in multiple domains as it handles complex optimization problems with discontinuities, non-differentials, noisy functions and functions with multi-modality. GA also supports parallel computations with obtaining Pareto front in a single run. Non-dominated sort GA-II (NSGA-II) is one of the MOEAs using GA strategy. NSGA-II implements non-dominated sort algorithm thus reducing the computational complexities. While sorting the parents and children, elitism is introduced in NSGA-II. In NSGA-II, to preserve the diversity and uniform spread of optimal front, a crowding distance (CD) operator is used. Chromosomes with better fitness are assigned highest ranks, and thus, they determine the domination [22].

Multi-objective PSO – crowding distance (MOPSO-CD) is one of the variants of MOPSO family. It uses PSO algorithm to handle MOO problems. It uses external archive/repository of non-dominated solutions to store the global best solutions, thus maintaining elitism. MOPSO used CD operator to select the global best solution and deletion method of the external archive. Along with CD operator, the mutation operator is used to maintain diversity amongst the solutions of the external archive. The non-dominated solutions stored in the external archive are used to guide the particle search [23].

Hence due to these merits, NSGA-II and MOPSO-CD have been widely implemented to solve MOO problems.

Genetic algorithm

Genetic algorithm, invented by Holland [24,25], is a meta-heuristic optimization algorithm based on the principle of genetics and natural selection. As random numbers are

generated during the operation of genetic algorithms hence GA is stochastic algorithms. These random numbers generated determine the search result [24–26]. For multi-objective optimization, NGPM code (NSGA-II Program in Matlab) is used [27,28]. NGPM is the implementation of NSGA-II (Non-dominated Sort Genetic Algorithm) in Matlab.

Firstly, non-dominated sorting is done using NSGA-II by comparing each individual with remaining solutions of a population [22] and thus, all non-dominated solutions and non-dominated fronts are identified and ranked. For rank 1 individuals, fitness value 1 is assigned. For rank 2 individuals, fitness value 2 is assigned and so on [22].

A new parameter, Crowding Distance (CD), is introduced by NSGA-II [22]. CD is the measure of diversity of individuals in the non-dominated population. After completing the sorting, CD is assigned to each individual, front-wise. More the CD more is the diversity in the population. Individuals in the boundary are always selected as they have assigned infinite CD.

From the non-dominated front, parents are selected on the basis of tournament selection and comparing the CD. New offsprings are created using crossover operator and mutation operator. New offsprings and current population (parents) are combined to generate a new population. Selection is carried out for next generation individuals.

The binary tournament selection method is used by NSGA-II to handle constraints. In this method, a solution either feasible or infeasible is decided by comparing with other solution. Here constrained dominate solution between two solutions is identified by using following rule –

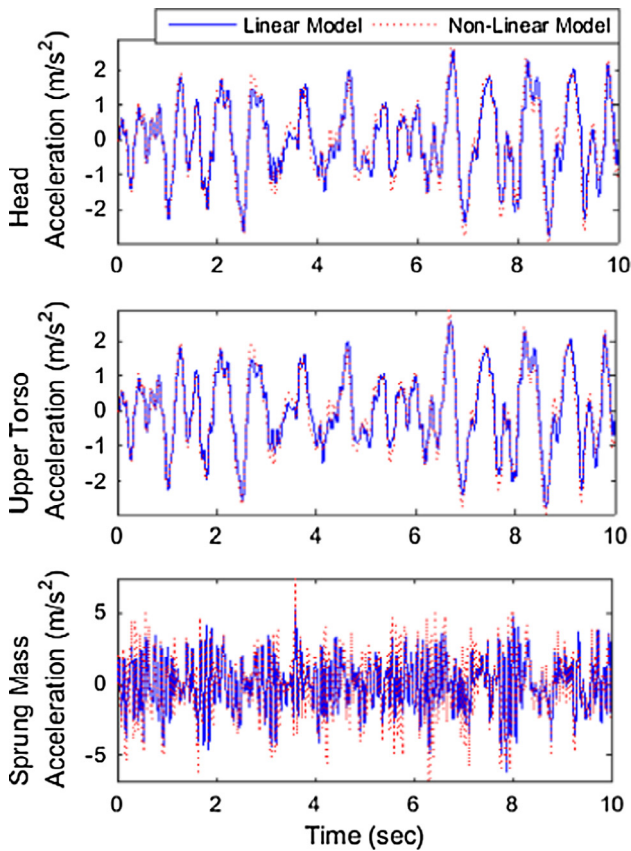


Fig. 1d Class C road input – linear and nonlinear quarter model – time response.

A solution i is said to be constrained dominate a solution j if

- (a) i is a feasible solution, whereas j is not.
- (b) Both solutions, i and j , are infeasible; however, i has overall constraint violation smaller as compared to j .
- (c) i and j solutions are feasible, but i dominates j .

Here, the number of generations is used as stoppage criterion. Fig. 2a explains the flow chart of GA algorithm implemented for multi-objective optimization.

MOPSO-CD

PSO algorithm proposed by Eberhart and Kennedy [29] was inspired by the social behaviour of birds’ flock searching randomly for food. While searching for food, instead of knowing the exact location of food, birds know their current location from food, and birds searches the bird which is closest to the food. Thus, PSO is a population-based algorithm where each bird is known as a particle. The particle flies through the solution space (or search space) to search the optimal solution. Each particle flies through the search space with a velocity which is determined according to the flying experience of bird’s own flying and its flock. All the particles have objective function value as per objective function. Each particle updates its position in search space based on its current location and previous best location (also called as p_{best}) and best location of the whole population (flock) (also called as g_{best}), current velocity.

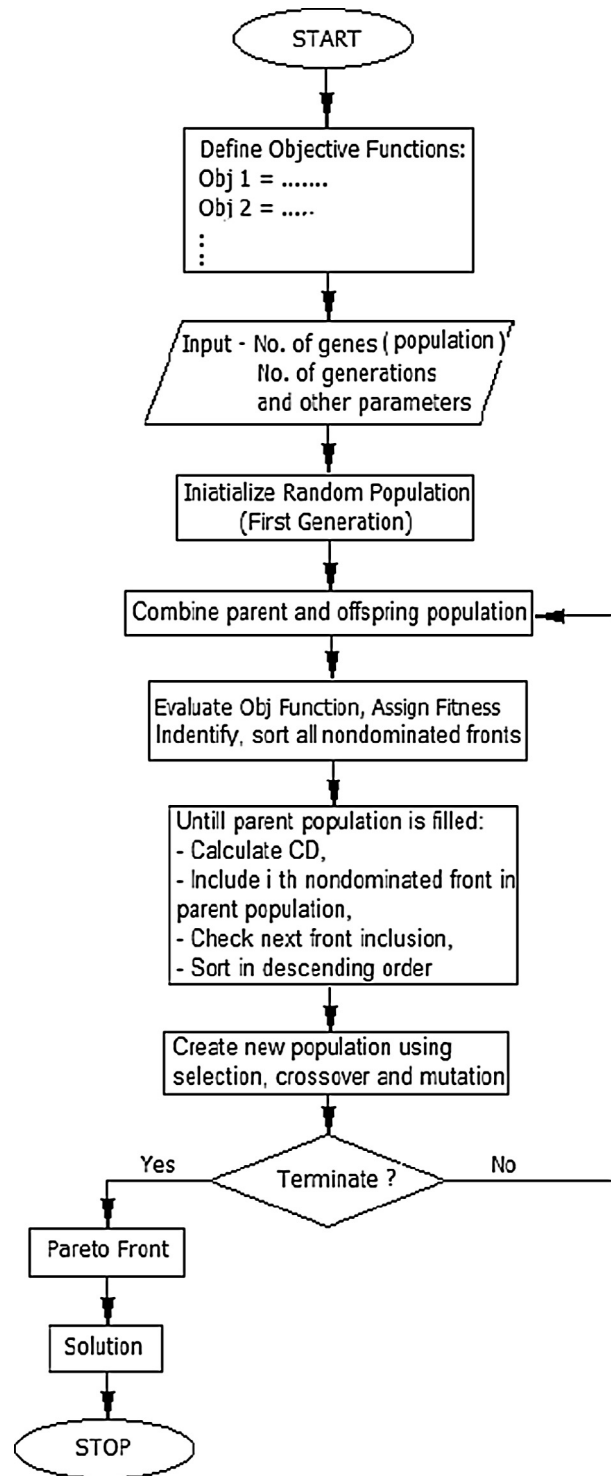


Fig. 2a Flow chart – GA.

In PSO algorithm, particles’ initial positions and initial velocities are randomly initialized.

The new velocity and new position of every particle can be determined using following equations:

$$\left. \begin{aligned} v_{ij}^{t+1} &= wv_{ij}^t + c_1r_1(p_{best_{ij}}^t - x_{ij}^t) + c_2r_2(g_{best_{ij}}^t - x_{ij}^t) \\ z_{ij}^{t+1} &= z_{ij}^t + z_{ij}^{t+1} \end{aligned} \right\} \quad (2)$$

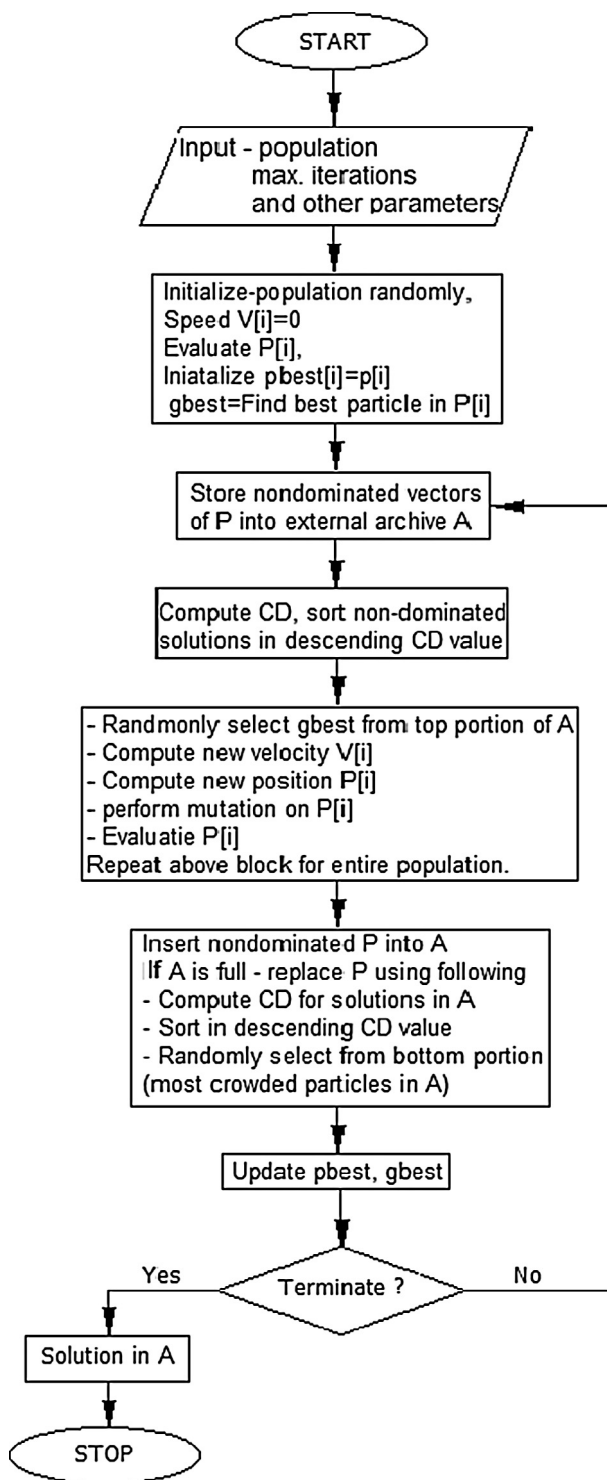


Fig. 2b Flow chart – PSO.

where w is inertia weight, c_1 and c_2 are acceleration coefficients and r_1 and r_2 are the uniform random numbers in the range $[0, 1]$. The optimization is an iterative process and thus converges to the global optimal solution.

In single objective optimization, it is easy to calculate p_{best} and g_{best} values, as compared to multi-objective optimization. Due to multi-objective nature of the problem and conflict

between the objectives, it is quite difficult to calculate the p_{best} and g_{best} values. It is impossible for all objective functions to reach maximum values or minimum value at the same time. Thus, in multi-objective PSO (MOPSO) uses the Pareto ranking scheme to take care the multi-objective problem. In MOPSO non-dominated solutions are stored in the archive where the historical records of best solutions are obtained [30].

MOPSO-CD [23] algorithm includes crowding distance (CD), similar to NSGA-II, computation mechanism in the PSO algorithm to solve multi-objective problems. The CD mechanism is used in selection of g_{best} and in deletion of an external archive of non-dominated solutions. To maintain diversity in the non-dominated archive, the mutation operator is used along with CD mechanism. The global best, g_{best} , is selected from those having highest CD values. The non-dominated solutions are moved in an external repository; A. External repository A is having solutions with least crowded objective space. Fig. 2b explains the flow chart of PSO optimization algorithm.

Constraint handling in MOPSO-CD

In multi-objective constrained optimization, the key issue is the constrained handling technique. Here, penalty function method is used for constrained handling as it is simple yet has good convergence [31].

Let us consider the multi-objective problem as follows:

$$\text{Minimize } F = [f_1(x), f_2(x), \dots, f_n(x)] \tag{3}$$

Subject to, $g_i(x) \leq 0, i = 1, 2, \dots, p$
 $h_j(x) = 0, j = 1, 2, \dots, q$

where $x = [x_1, x_2, \dots, x_m]$ is a decision variable in a decision space X .

In this paper, only inequality constraints are considered for optimization. Here, for constraint handling in the multi-objective optimization problem, the degree of violation of constraint is used in penalty function method. Each particle is checked for the constraint violation. Upon violation of constraint by particle x , the degree of constraint violation is defined as

$$f_p(x) = f(x) + \sum_{i=1}^m C \delta_i \tag{4}$$

where δ_i = extent of constraint violation and $\delta_i = 0$ if a constraint is not violated when i th constraint is satisfied. C = Penalty.

Objective functions

One of the key factors in optimization problems is to choose proper objective functions. As stated earlier, body parts respond to a much greater extent as compared to seat response. Hence, suspension system is aimed to optimize considering responses such as RMS head acceleration, Vibration dose value (VDV) at head, the amplitude ratio of head RMS acceleration to seat RMS acceleration, the amplitude ratio of upper torso RMS acceleration to seat RMS acceleration, and crest factor as these are the most important factors which affect the driver’s health. Along with these objective functions, suspension space deflection and dynamic tyre force are also included as objective functions to form a multi-objective optimization problem.

RMS head acceleration: As per ISO 2631-1 [32], RMS head acceleration is given by

$$A_{wh} = \left\{ \frac{1}{T} \int_0^T [a_{wh}(t)]^2 dt \right\}^{\frac{1}{2}} \quad (5)$$

A major portion of the vibration experienced by the occupants of an automobile enters the body through the seat [33,34]. Whole-body vibrations, mostly affect the human body, are characterized by vertical vibrations transmitted to the buttocks and back of the occupant along the vertebral axis via the base. The health risk increases as the exposure time to vibrations increases. Hence is it necessary to measure the whole body vibrations. As per ISO 2631-1 [32], VDV is one measure for whole body vibrations. VDV is also called as fourth power vibration dose. VDV is the method of assessing the cumulative effect (dose) of the vibration.

Vibration Dose Value (VDV): VDV is the fourth power of acceleration time histories. It is expressed as follows:

$$VDV_h = \left\{ \int_0^T [a_{wh}(t)]^4 dt \right\}^{\frac{1}{4}} \quad (6)$$

Crest Factor (CF): It is defined as the ratio of maximum head acceleration to the RMS head acceleration [32].

$$CF = \text{Max}(a_h) / \left\{ \frac{1}{T} \int_0^T [a_{wh}(t)]^2 dt \right\}^{\frac{1}{2}} \quad (7)$$

Amplitude ratio of head RMS acceleration to seat RMS acceleration (AR_h): It defined as the ratio of head RMS acceleration to seat RMS acceleration.

$$AR_h = \left\{ \frac{1}{T} \int_0^T [a_h(t)]^2 dt \right\}^{\frac{1}{2}} / \left\{ \frac{1}{T} \int_0^T [a_s(t)]^2 dt \right\}^{\frac{1}{2}} \quad (8)$$

Amplitude ratio of upper torso RMS acceleration to seat RMS acceleration (AR_ut): It is defined as the ratio of upper torso RMS acceleration to seat RMS acceleration.

$$AR_{ut} = \left\{ \frac{1}{T} \int_0^T [a_{ut}(t)]^2 dt \right\}^{\frac{1}{2}} / \left\{ \frac{1}{T} \int_0^T [a_s(t)]^2 dt \right\}^{\frac{1}{2}} \quad (9)$$

Suspension travel: Suspension travel is characterized by the relative travel between the sprung mass and unsprung mass. Due to random input, RMS suspension space travel is taken as one of the objective functions.

$$\text{Suspension Travel} = x_s - x_{us} \quad (10)$$

$$\text{RMS Suspension Travel} = \left\{ \frac{1}{T} \int_0^T [(x_s(t) - x_{us}(t))]^2 dt \right\}^{\frac{1}{2}} \quad (11)$$

Dynamic tyre force: Dynamic tyre force is related to tyre deflection. Due to random nature of input RMS of tyre deflection is next objective function.

$$\text{Tyre Deflection} = x_{us} - x_r \quad (12)$$

$$\text{RMS Tyre Deflection} = \left\{ \frac{1}{T} \int_0^T [(x_{us}(t) - x_r(t))]^2 dt \right\}^{\frac{1}{2}} \quad (13)$$

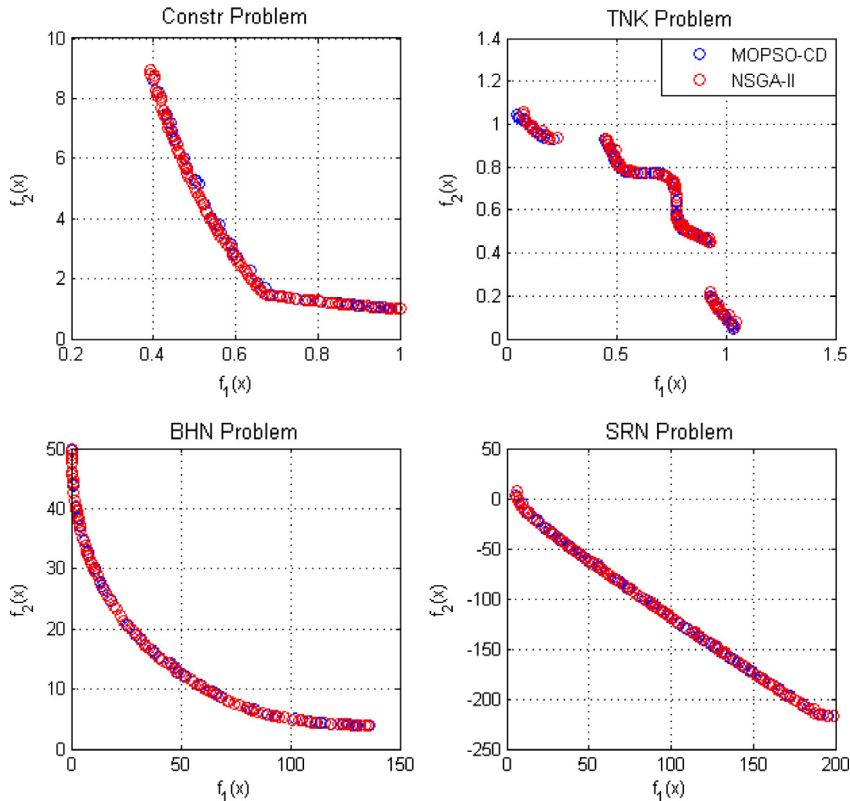


Fig. 3a Pareto front for benchmark problems.

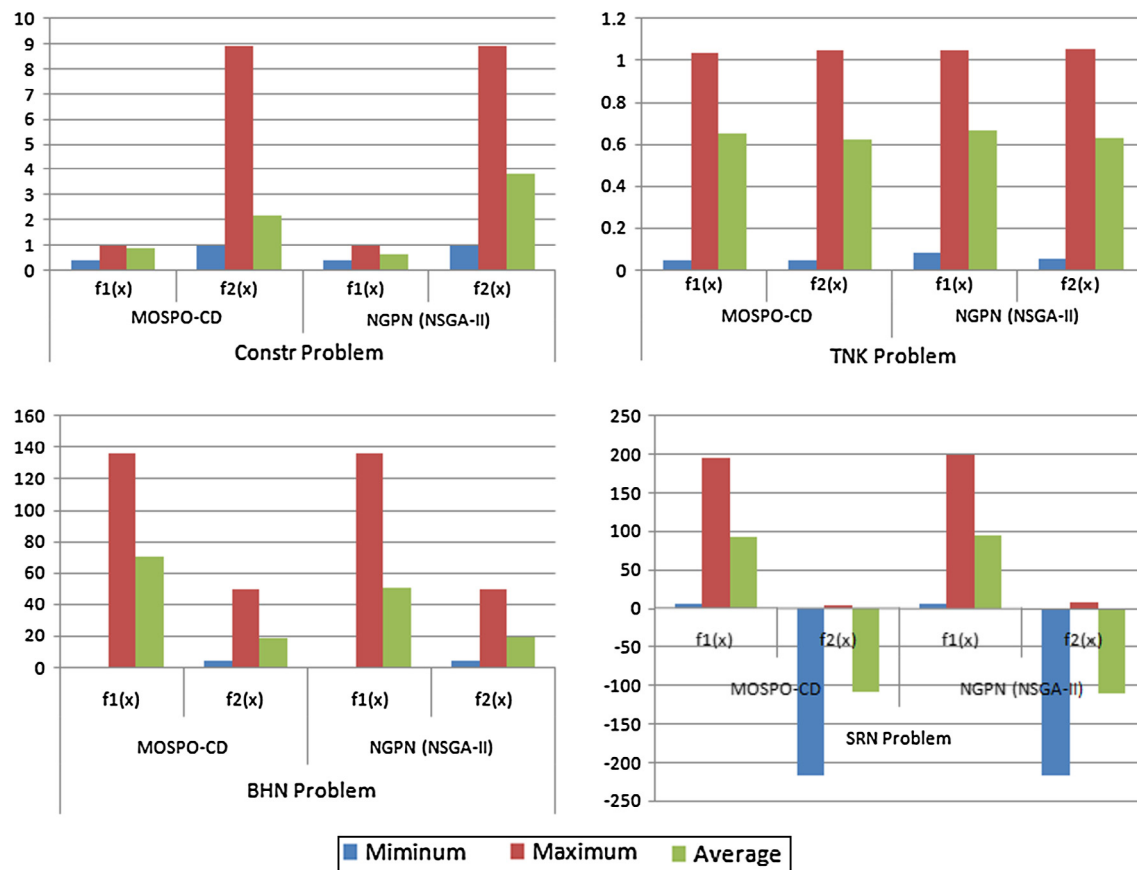


Fig. 3b Comparison of benchmark functions.

According to Baupal and et al. [8], at least, 125 mm of suspension travel is required and maximum seat acceleration should not increase 4.5 m/s^2 so as to avoid hitting the suspension stop. To minimize dynamic tyre forces, maximum tyre deflection should not increase 0.058 m. These parameters are included as constraints in the optimization problem.

The formulation of optimization problem is as follows:

$$f_{\text{obj}1} = \text{Minimize } (VDV_h)$$

$$f_{\text{obj}2} = \text{Minimize } (A_{\text{wh}})$$

$$f_{\text{obj}3} = \text{Minimize } (CF)$$

$$f_{\text{obj}4} = \text{Minimize } (AR_h)$$

$$f_{\text{obj}5} = \text{Minimize } (AR_{\text{ut}})$$

$$f_{\text{obj}6} = \text{Minimize } (\text{RMS suspension travel})$$

$$f_{\text{obj}7} = \text{Minimize } (\text{RMS tyre deflection})$$

Table 2 Benchmark function values.

Benchmark problem	Optimization algorithm	Objective function	Minimum value	Maximum value	Average value	Elapsed time (s)
Constr problem	MOPSO-CD	$f_1(x)$	0.391933	1	0.834189	11.11693
		$f_2(x)$	1	8.929097	2.161154	
	NGPM (NSGA-II)	$f_1(x)$	0.391348	1	0.616499	36.02496
		$f_2(x)$	1	8.91946	3.798027	
TNK problem	MOPSO-CD	$f_1(x)$	0.048698	1.036299	0.647836	10.97732
		$f_2(x)$	0.048177	1.046548	0.623831	
	NGPM (NSGA-II)	$f_1(x)$	0.078051	1.04836	0.666922	40.06497
		$f_2(x)$	0.056232	1.05603	0.632637	
BHN problem	MOPSO-CD	$f_1(x)$	0	136	70.43662	9.913939
		$f_2(x)$	4	50	18.52125	
	NGPM (NSGA-II)	$f_1(x)$	0	136	50.81124	28.55074
		$f_2(x)$	4	50	19.64545	
SRN problem	MOPSO-CD	$f_1(x)$	5.729107	195.7479	92.60403	7.154332
		$f_2(x)$	-217.471	3.609806	-108.957	
	NGPM (NSGA-II)	$f_1(x)$	5.99457	198.688	94.82053	19.75622
		$f_2(x)$	-216.96	7.87181	-110.502	

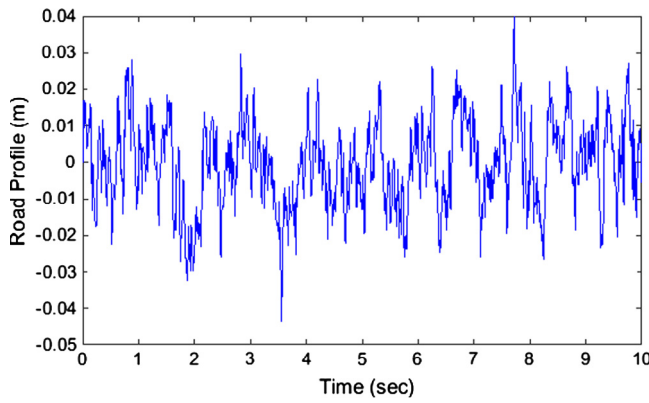


Fig. 4 Road surface (Class C, velocity 80 kmph).

Subject to constraints:

$$a_{\max, \text{seat}} \leq 4.5 \text{ m/s}^2, \max.(x_s - x_{us}) \leq 0.125 \text{ m}, \max.(x_{us} - x_r) \leq 0.058 \text{ m},$$

Search space:

During optimization, the design parameters are suspension spring stiffness; suspension damping and seat cushion parameters. The search space is:

$$k_s \in \pm 50\%k_s, c_s \in \pm 50\%c_s, [10] \text{ Hence, } k_s \in [11750, 35250], c_s \in [350, 1050], k_c \in [2500, 20000], c_c \in [131.59, 1649.03] [35]$$

Results and discussion

Test problems

To test the performance of NSGA-II and MOPSO-CD with penalty function, four benchmark problems are selected and simulated. Each benchmark function has two objective functions, two constraint functions and two design variables.

1. Constr problem:

$$\left. \begin{aligned} \text{Minimize } f_1(x) &= x_1 \\ \text{Minimize } f_2(x) &= (1 + x_2)/x_1 \end{aligned} \right\} \quad (14)$$

Subject to

$$\left. \begin{aligned} g_1(x) &= x_2 + 9x_1 \geq 6, \\ g_2(x) &= -x_2 + 9x_1 \geq 1 \end{aligned} \right\} \quad (15)$$

Design variables

$$x_1 \in [0.1, 1.0], x_2 \in [0, 5.0]$$

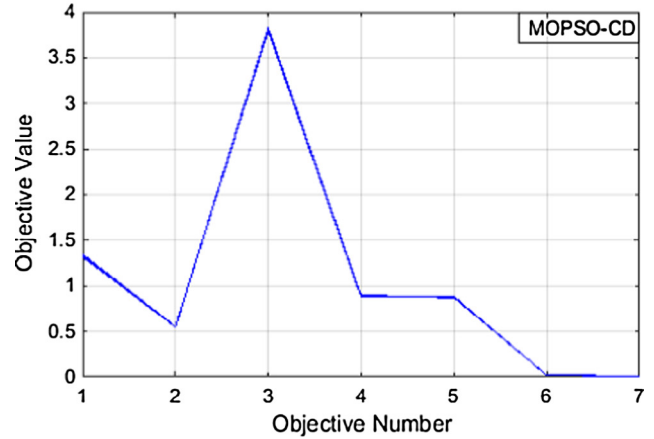
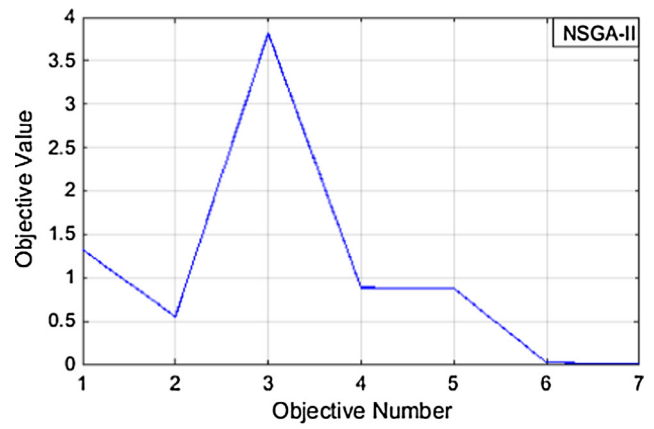


Fig. 5a Trade-off Front for NSGA-II and MOPSO-CD.

2. TNK problem

$$\left. \begin{aligned} \text{Minimize } f_1(x) &= x_1 \\ \text{Minimize } f_2(x) &= x_2 \end{aligned} \right\} \quad (16)$$

Subject to

$$\left. \begin{aligned} g_1(x) &= x_1^2 + x_2^2 - 1 - 0.1\cos(16 \arctan(x_1/x_2)) \geq 0, \\ g_2(x) &= (x_1 - 0.5)^2 + (x_2 - 0.5)^2 \leq 0.5 \end{aligned} \right\} \quad (17)$$

Design variables

$$x_1 \in [0, \pi], x_2 \in [0, \pi]$$

3. BHN problem

$$\left. \begin{aligned} \text{Minimize } f_1(x) &= 4x_1^2 + 4x_2^2 \\ \text{Minimize } f_2(x) &= (x_1 - 5)^2 + (x_2 - 5)^2 \end{aligned} \right\} \quad (18)$$

Table 3 Design variables range.

Design variable	Range	Size	
k_s	$35,250 - 11,750 = 23,500$	$2^{14} = 16,384 < 23,500 < 2^{15} = 32,768$	15 bits
c_s	$1050 - 350 = 700$	$2^9 = 512 < 700 < 2^{10} = 1024$	10 bits
k_c	$20,000 - 2500 = 17,500$	$2^{14} = 16,384 < 17,500 < 2^{15} = 32,768$	15 bits
c_c	$1649.03 - 131.59 = 1517.44$	$2^{10} = 1024 < 1517.44 < 2^{11} = 2048$	11 bits

Subject to

$$\left. \begin{aligned} g_1(x) &= (x_1 - 5)^2 + x_2^2 \leq 25, \\ g_2(x) &= (x_1 - 8)^2 + (x_2 + 3)^2 \geq 7.7 \end{aligned} \right\} \quad (19)$$

Design variables

$$x_1 \in [0, 5], \quad x_2 \in [0, 3]$$

4. SRN problem

$$\left. \begin{aligned} \text{Minimize } f_1(x) &= 2 + (x_1 - 2)^2 + (x_2 - 2)^2 \\ \text{Minimize } f_2(x) &= 9x_1 - (x_2 - 1)^2 \end{aligned} \right\} \quad (20)$$

Subject to

$$\left. \begin{aligned} g_1(x) &= x_1^2 + x_2^2 \leq 225, \\ g_2(x) &= x_1 - 3x_2 + 10 \leq 0 \end{aligned} \right\} \quad (21)$$

Design variables

$$x_1 \in [-20, 20], \quad x_2 \in [-20, 20]$$

Both algorithms are run using following parameters:

NSGA-II: Population size = 100, number of generations = 100, thus having 10,000 evaluation count.

MOSPO-CD: Number of particles 100 with Maximum number of particles in repository A = 100 [30], and Maximum evaluation = 10,000.

Both algorithms are simulated in Matlab/Simulink environment. Pareto front and results are shown graphically in Figs. 3a and 3b respectively. Pareto fronts of both algorithms are in close agreement with each other. Results are also tabulated in Table 2. The table shows minimum value, the maximum value and the average value of each benchmark problem/function from the set of solutions of 100. Also, Table 2 shows elapsed time for each problem.

In each benchmark problem, both objective functions are of minimization nature. From Table 2 and Fig. 3b, for Constr problem it is observed that minimum, maximum, and average function values are less for NSGA-II as compared to MOPSO-CD. However, the average function value of $f_2(x)$ function is

Table 4 Objective function values.

Objective functions	NSGA-II	MOPSO-CD	Classical
VDV _h	1.3178	1.3171	3.1028
RMS A_{wh}	0.5491	0.5481	1.3504
CF	3.8099	3.7961	3.8418
STHT	0.8804	0.8875	1.1058
AR	0.8721	0.8712	1.1033
RMS suspension space	0.0189	0.0196	0.02248
RMS tyre deflection	0.0108	0.0114	0.0100
<i>Constraints</i>			
Maximum a_h	2.8195	2.8224	5.5455
Suspension space deflection	0.0593	0.0633	0.06424
Tyre deflection	0.0364	0.0370	0.0344
Optimization time (s)	9345.2454	8858.4179	-

Table 5 Design variables.

	k_s	c_s	k_c	c_c
NSGA-II	11,750	546.4720	2510	1509.73
MOPSO-CD	11,750	542.1716	2500.2333	1500

much less for MOPSO-CD algorithm as compared to NSGA-II. In case of TNK problem, it observed that minimum, maximum and average function values are less for MOPSO-CD as compared to NSGA-II. For BHN problem, minimum and maximum function values are same for both algorithms. However, the average value of $f_1(x)$ function is greater for MOPSO-CD algorithm as compared to NSGA-II, whereas the average value of $f_2(x)$ function is smaller for MOPSO-CD algorithm as compared to NSGA-II. For SRN problem, it observed that minimum, maximum and average function values are less for MOPSO-CD as compared to NSGA-II. From Table 2, it is clear that MOSPO-CD takes much lesser computation time as compared to NSGA-II algorithm for benchmark problems.

Validation on a nonlinear quarter car

Multi-objective optimization of nonlinear quarter car model is simulated in Matlab/Simulink® environment using NSGA-II and MOPSO-CD algorithms.

The stationary road roughness is effectively described by power spectral density (PSD) [36]. When a car moves at a constant velocity u , the road roughness can be viewed as a stationary process in space domain, and the PSD of the road disturbance input can be expressed by

$$Sq(n) = Sq(n_o) \left(\frac{n}{n_o} \right)^{-\omega} \quad (22)$$

where $Sq(n)$ is the road PSD, n is the spatial frequency, n_o is the reference spatial frequency and $n_o = 0.1(\text{cycles/m})$. $Sq(n_o)$ is the coefficient of road roughness, and ω is waviness and is generally $\omega = 2$.

In frequency domain, PSD can be expressed as

$$S_q(\omega) = S_q(\Omega_o) v / (\omega^2 + \omega_o^2) \quad (23)$$

where ω_o is the lowest cut-off angular frequency and $\omega_o = 2\pi f_o = 2\pi v n_o$.

The differential equation of road roughness can be expressed as [36]

$$\dot{x}_r(t) + 2\pi n_o v x_r(t) = \sqrt{S_q(n_o) v} w(t) \quad (24)$$

Eq. (24) is modelled in Simulink environment to model the road surface. Input road condition is modelled as class C road (average road) with degree of road roughness $512 \times 10^{-6} \text{ m}^2/(\text{cycle/m})$ [36,37]. The vehicle is travelling with velocity of 80 kmph. Fig. 4 represents the class C road surface.

For GA, the range of design variable k_s is $(35,250 - 11,750 =) 23,500$. Thus, design variable k_s needs to be divided into 23,500 equal range of size. Hence $2^{14} = 16,384 < 23,500 < 2^{15} = 32,768$ i.e. 15 bits are required to store value of design variable k_s in the chromosome. Similarly for other design variables, the bit required is tabulated in Table 3.

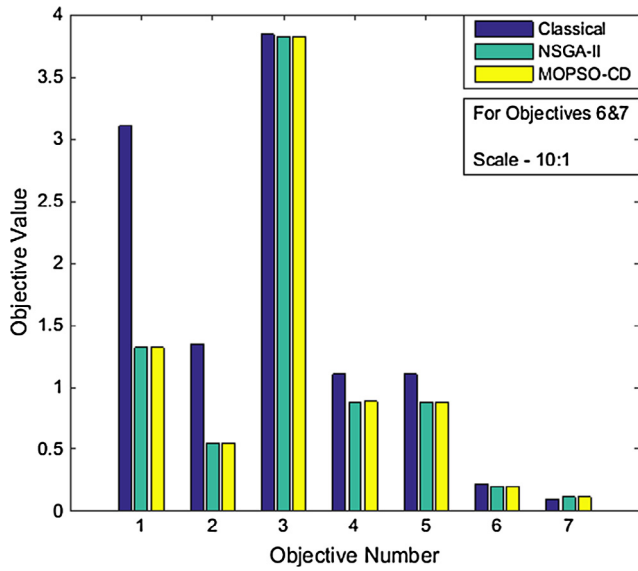


Fig. 5b Objective Function Values corresponding to minimum Aw.

Hence, the total length of chromosome or gene is 15 + 10 + 15 + 11 = 51 bits are required where first 15 bits are required for k_s , next 11 bits are required for c_s , next 15 bits are required for k_c and next 11 bits are required for design variable c_c .

A lot of work is done on determining the optimum population size for GA based optimization. Rosenthal and Borschbach [38] in their study concluded that the best performance for NSGA-II is achieved with a population size ranging from 70 to 100. Hernandez-Diaz et al. [39] experimentally found that NSGA-II needs minimum population size of 52 to reach a good performance. Reeves and Rowe [40] derived a formula based on the principle that, in the search space every point should be reachable from the initial population. In GA, the initial population is randomly generated. Therefore, the probability that at least one allele is present at each locus is given by equation:

$$P_2^* = \left(1 - (1/2)^{N-1}\right)^{l_s} \tag{25}$$

where N = population size and l_s = string length

Using exponential function approximation, the population size is given by equation:

$$N \approx [1 + \log(-l_s / \ln P_2^*) / \log 2] \tag{26}$$

According to Eq. (26), population size 17 is sufficient for the string of length 50 to exceed the probability of 99.9%.

According to Alander [41], population size is given by relation:

$$l_s \leq N \leq 2l_s.$$

Thus selecting population size of 100 for optimization and the stoppage criterion is the number of generations and is equal to 100 generations.

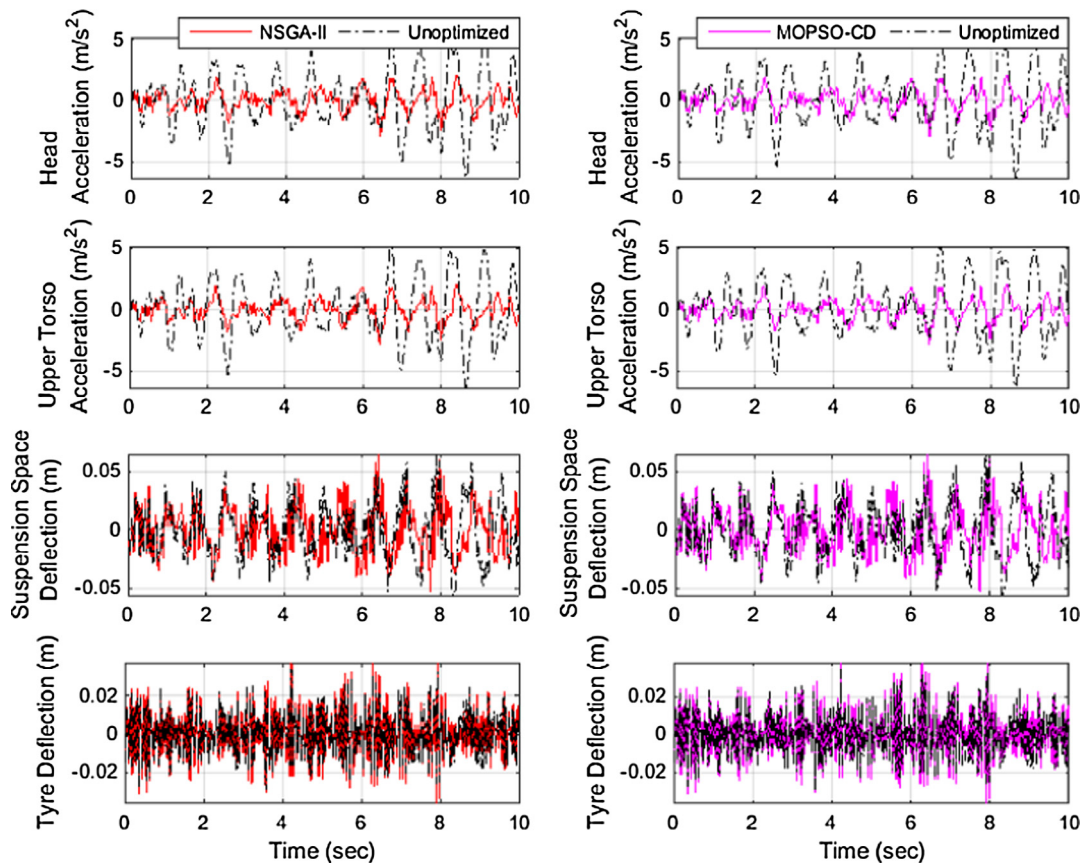


Fig. 5c Time response of quarter car seat-suspension-driver model.

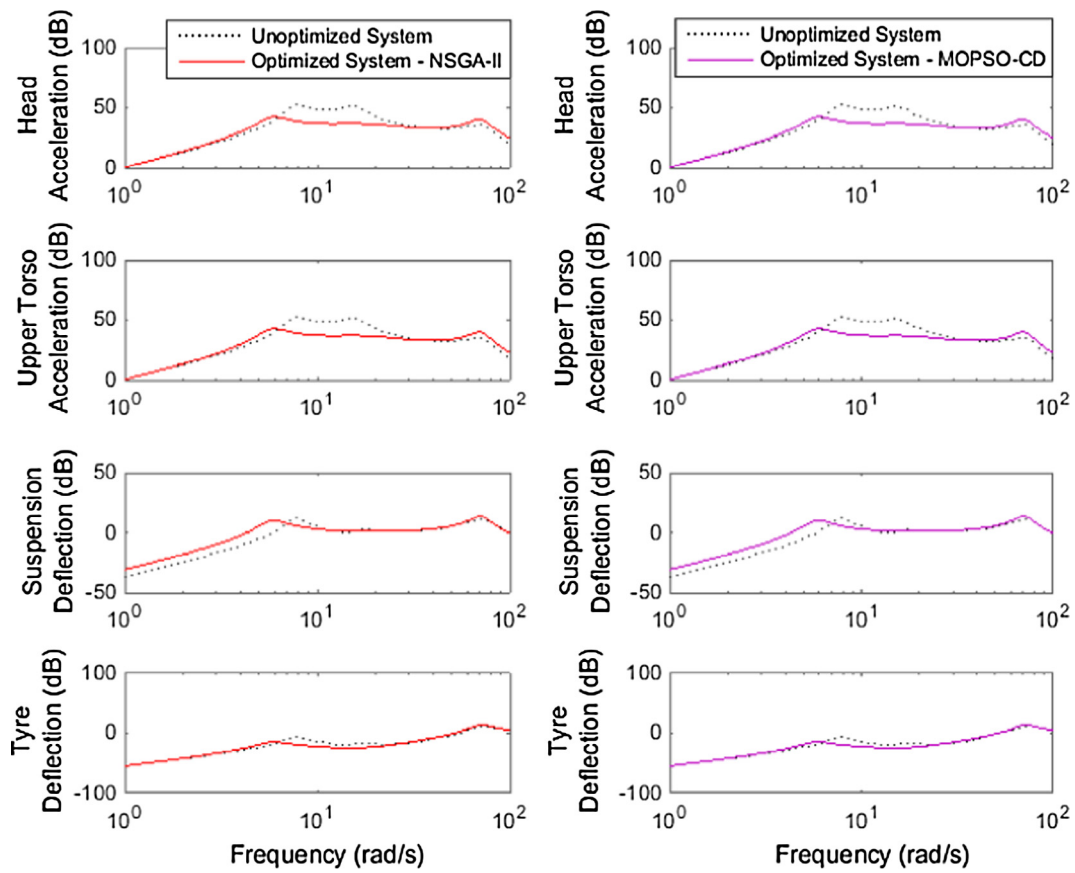


Fig. 5d Frequency response of quarter car seat–suspension–driver model.

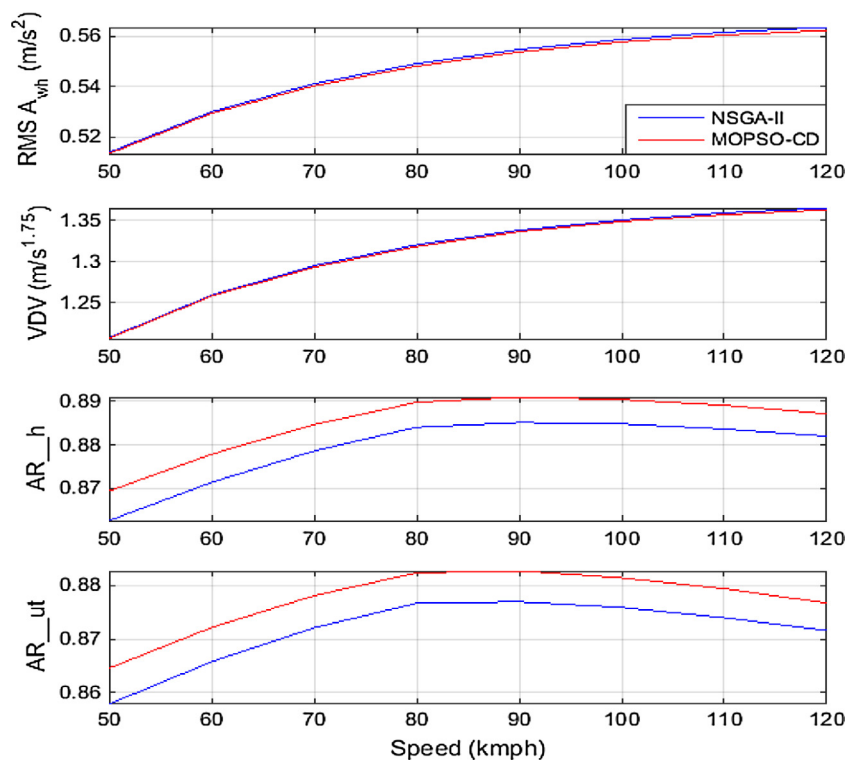


Fig. 6a Performance of optimized variables at various speeds.

In MOPSO-CD, algorithm 100 particles are used with a repository of size 100 to store non-dominated solutions and a maximum number of evaluations 100,000 to stop the algorithm [30].

Multi-objective optimization of nonlinear quarter car suspension driver system is established using GA and PSO to search optimum parameters of the suspension system (i.e. spring stiffness and damping coefficient) and cushion (i.e. cushion material stiffness and damping). The aim was to minimize VDV, RMS sprung mass acceleration, crest factor, AR_h, AR_{ut}, suspension space deflection and tyre deflection.

Fig. 5a shows the trade-off fronts obtained for NSGA-II and MOPSO-CD optimization algorithm with four design variables i.e. k_s , c_s , k_c and c_c . Next step is to invoke the decision procedure to select a set of design variables from given sets of design variables. In this case, 100 sets of design variables are available for NSGA-II as well as MOPSO-CD algorithm approach, as population size is 100 for NSGA-II algorithm and repository size is 100 for the MOPSO-CD algorithm. This gives the designer more flexibility to choose a particular set of design variables as a solution for further analysis.

Hence, from the 100 sets of design objective functions, minimum value of each objective function is tabulated in Table 4 for both algorithms. Table 4 also represents the objective function values for the classical parameter.

To represents the results more clearly, design variables corresponding to the minimum value of RMS A_{wh} from Table 4 are selected for further analysis. The design variables correspond to the minimum value of RMS A_{wh} are tabulated in Table 5. The comparison of objective functions corresponding to minimum RMS A_{wh} for NSGA-II and MOPSO-CD with classical values is shown in Fig. 5b. From Fig. 5b, it is observed that RMS head acceleration and VDV at the head are very less for optimized variables (i.e. NSGA-II and MOPSO-CD algorithm) as compared to classical values. But there is a slight reduction in crest factor of optimized variables as compared to classical variables. Although the crest factors are nearly the same for optimized variables and the classical

one, still RMS head acceleration is very less for optimized variables thus providing good ride over classical one. The AR_h and AR_{ut} are reduced by 20% each for NSGA-II algorithm. Also, for MOPSO-CD algorithm, the reduction in AR_h and AR_{ut} is 19% and 20% respectively. Hence, optimized parameters provide better ride comfort and health by reducing RMS head acceleration and VDV at head, AR at head and upper torso.

The responses are simulated for Class C road at 80 kmph vehicle speed. Fig. 5c shows simulation responses of head acceleration, upper torso acceleration, suspension space deflection and tyre deflection for optimized design variables corresponding to the minimum value of A_{wh} along with classical values. In Fig. 5c, it is observed that head acceleration, upper torso acceleration of driver is considerably improved by optimized suspension-seat system.

Fig. 5d shows the frequency response of un-optimized parameters and optimized parameters using NSGA-II and MOPSO-CD algorithms. It is observed that head acceleration gain, upper torso acceleration gain, suspension deflection gain and tyre deflection gains are on the lower side for optimized NSGA-II and MOPSO-CD parameters compared to un-optimized parameters.

To check the performance on varying speed, optimized variables (shown in Table 5) are further simulated on class C road surface for speed ranging from 50 to 120 kmph. It is observed that RMS head acceleration increases with increase in speed. Maximum RMS head acceleration is 0.5536 m/s² and 0.5623 m/s² at 120 kmph for NSGA-II and MOPSO-CD, respectively. A similar trend is observed for VDV at the head, and it increases with increase in speed. Maximum VDV at the head is 1.3653 m/s^{1.75} and 1.3631 m/s^{1.75} at 120 kmph for NSGA-II and MOPSO-CD, respectively. Refer Fig. 6a.

Amplitude ratio AR_h and Amplitude ratio AR_{ut} also increase with increase in speed from 50 to 90 kmph. But, from 90 kmph slight decrease in both ratios is observed. Maximum AR_h is 0.8851 and 0.8908 at 90 kmph for NSGA-II and

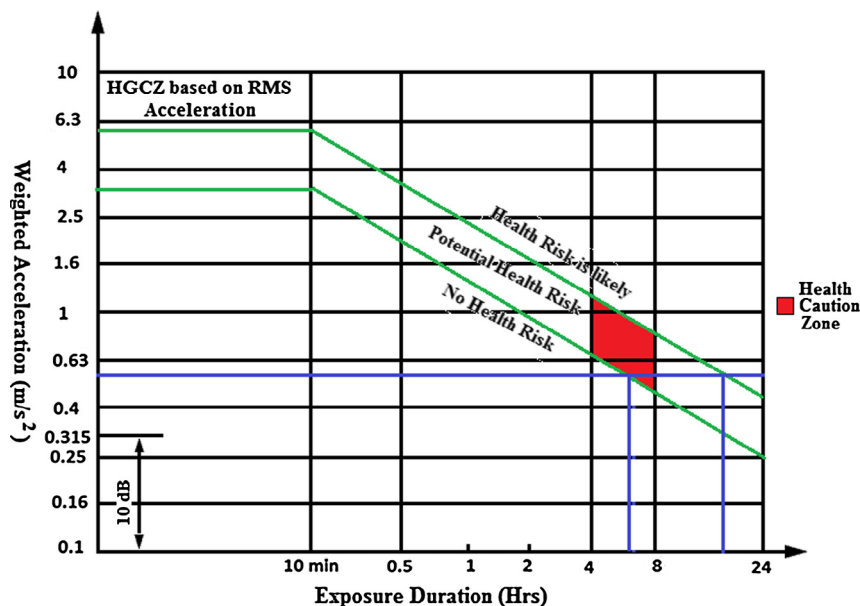


Fig. 6b Annexure B – ISO 2631-1 (Health Guidance Caution Zone, HGCZ) [32].

Table 6 Time limits as per Health Guidance Caution Zone (HGCZ) as per ISO – 2631-1.

Speed (kmph)	NSGA-II (Class C road)				MOPSO-CD (Class C road)			
	A_{wh} (m/s ²)	Vibration exposure limit (h)			A_{wh} (m/s ²)	Vibration exposure limit (h)		
		NHR	PHR	LHR		NHR	PHR	LHR
50	0.5138	7	7–18	18–24	0.5133	7	7–18	18–24
60	0.5300	6	6–17	17–24	0.5293	6	6–17	17–24
70	0.5411	6	6–17	17–24	0.5403	6	6–17	17–24
80	0.5491	6	6–17	17–24	0.5480	6	6–17	17–24
90	0.5547	6	6–17	17–24	0.5537	6	6–17	17–24
100	0.5587	6	6–17	17–24	0.5576	6	6–17	17–24
110	0.5616	6	6–17	17–24	0.5604	6	6–17	17–24
120	0.5635	6	6–17	17–24	0.5623	6	6–17	17–24

MOPSO-CD, respectively. At 120 kmph AR_h is 0.8819 and 0.8870 for NSGA-II and MOPSO-CD, respectively. Similarly, maximum AR_{ut} is 0.8770 and 0.8828 at 90 kmph for NSGA-II and MOPSO-CD, respectively. At 120 kmph AR_{ut} is 0.8716 and 0.8768 for NSGA-II and MOPSO-CD, respectively.

The factors associated with the assessment of health risk are the magnitude of vibration and duration of vibration. In this study, the magnitude of vibration is determined according to frequency weighted RMS head acceleration as per ISO 2631-1 [32] standard. Annexure B of ISO 2631-1 provides a graphical representation of Health Guidance Caution Zone (HGCZ). The graph has two criterions for assessment of health prediction – first is based on exposure duration and vibration magnitude as per RMS value of A_w and second based on VDV. Here, the first criterion is used to assess prediction of health risk and shown in Fig 6b. This criterion is divided into three different exposure levels – no health risk (NHR), potential health risk (PHR) and likely health risk (LHR), refer Fig. 6b.

Table 6 represents RMS A_{wh} for 10-min duration. For 10 min period, it is observed that the RMS A_{wh} values lie well within the NHR zone for both optimization methods. Fig. 6b shows the RMS head acceleration for 120 kmph vehicle speed, represented by a blue line. From Fig. 6b, for 0.5635 m/s² RMS head acceleration, vibration exposure limit is up to 6 h for NHR and 6–17 h for PHE and 17–24 h is for LHR. Table 6 shows the time duration of both optimization algorithms according to exposure levels as per ISO 2631-1 criterion. Thus, optimized variables improve ride and health criterions.

Conclusions

This paper presents multi-objective optimization of Nonlinear Quarter Car Seat Suspension system with a driver model. An eight DoF model consisting of 2 DoF nonlinear quarter car model having quadratic nonlinearities in tyre and cubic nonlinearity in suspension spring, 4 DoF driver biomechanical model, seat frame and the seat cushion are developed and optimized.

In optimum design problem comfort and health criterion consisting of VDV at the head, RMS head acceleration, crest factor, AR_h, AR_{ut}, along with stability criterions consisting of suspension space and tyre deflection are used as objective functions. ISO 2631-1 methodology is adopted to assess the

objective functions such as RMS head acceleration, VDV at head and crest factor.

Optimization of the car suspension–seat–driver system is successfully implemented using NSGA-II and MOPSO-CD with penalty function algorithms. The MOPSO-CD algorithm takes less computation time as compared to NSGA-II for optimization.

Numerical simulations are presented for optimum design variables of a quarter car suspension–seat–driver system obtained by implementing NSGA-II and MOPSO-CD algorithms. Results of a quarter car travelling over a Class C road (average road) at speed 80 kmph are presented to show its performance. For class C road, RMS head acceleration and VDV at head increase with increase in speed. Simulation result shows that optimum design variables improve ride comfort and health criterions over classical design variables.

Conflict of interest

The authors have declared no conflict of interest.

Compliance with Ethics Requirements

This article does not contain any studies with human or animal subjects.

Acknowledgements

The first author likes to thank the Management of Ahmednagar Jilha Maratha Vidya Prasarak Samaj, Ahmednagar, and the Principal of SCSMCoE, Ahmednagar, for kind support and encouragement to carry this research work. Also, the first author likes to thank the Savitribai Phule Pune University (Formerly University of Pune), Pune and BCUD for sanctioning QIP program.

References

- [1] Wong JY. *Theory of ground vehicles*. 3rd ed. NY: John Wiley & Sons Inc; 2001. p. 431–83.
- [2] Gobbi M, Mastinu G. Analytical description and optimization of the dynamic behaviour of passively suspended road vehicles. *J Sound Vib* 2001;245(3):457–81.

- [3] Verros G, Natsiavas S. Design optimization of quarter-car models with passive and semi-active suspensions under random road excitation. *J Vib Control* 2005;11:581–606.
- [4] Özcan D, Sönmez Ü, Güvenç L. Optimisation of the nonlinear suspension characteristics of a light commercial vehicle. *Int J Vehicular Technol* 2013;2013:1–16.
- [5] Molina-Cristobal A, Papageorgiou C, Parks G, Smith M, Clarkson P. Multi-objective controller design: evolutionary algorithms and bilinear matrix inequalities for a passive suspension. In: *Proceedings of 13th IFAC workshop on control applications of optimization*, France. Dover; 2006. p. 386–91.
- [6] Chi Z, He Y, Naterer G. Design optimization of vehicle suspensions with a quarter-vehicle model. *Trans CSME* 2008;32(2):297–312.
- [7] Gomes H. A Swarm Optimization Algorithm for Optimum Vehicle Suspension Design. In: *Proceedings of 20th international congress of mechanical engineering*, Brazil. p. 1–10.
- [8] Bauml A, McPhee J, Calamai P. Application of genetic algorithms to the design optimization of an active vehicle suspension system. *Comput Methods Appl Mech Eng* 1998;163:87–94.
- [9] Kuznetsov A, Mammadov M, Sultan I, Hajilarov E. Optimization of a quarter-car suspension model coupled with driver biomechanical effects. *J Sound Vib* 2011;330:2937–46.
- [10] Gundogdu O. Optimal seat and suspension design for a quarter car with driver model using genetic algorithm. *Int J Ind Ergonom* 2007;37:327–32.
- [11] Badran S, Salah A, Abbas W, Abouelatta O. Design of optimal linear suspension for quarter car with human model using genetic algorithms. *Res Bull Jordan ACM* 2012;II(II):42–51.
- [12] Patil M, Palanichamy M. Minimization of human body responses to low frequency vibration: application to tractor and trucks. *Math Mod* 1985;6:421–42.
- [13] McGee C, Haroon M, Adams D, Luk Y. A frequency domain technique for characterizing nonlinearities in a tire-vehicle suspension system. *J Vib Acoust* 2005;127:61–76.
- [14] Zhu Q, Ishitobi M. Chaotic vibration of a nonlinear full-vehicle model. *Int J Solids Struct* 2005;43:747–59.
- [15] Lixia J, Wanxiang L. Chaotic vibration of a nonlinear quarter-vehicle model. In: *Proceedings of IEEE vehicle power and propulsion conference*, China. p. 1–4.
- [16] Coermann R. The mechanical impedance of the human body in sitting and standing positions at low frequencies. *Hum Factors* 1962;4:227–53.
- [17] Wei L, Griffin J. The prediction of seat transmissibility from measures of seat impedance. *J Sound Vib* 2008;214(1):121–37.
- [18] Suggs C, Abrams C, Stikeleather L. Application of a damped spring-mass human vibration simulator in vibration testing of vehicle seats. *Ergonomics* 1969;12:79–90.
- [19] Wan Y, Schimmels J. A simple model that captures the essentials dynamics of a seated human exposed to whole body vibrations. *ASME Adv Bioeng* 1995;31:333–4.
- [20] Boileau P, Rakheja S. Whole-body vertical biodynamic response characteristics of the seated body biodynamic response under vertical vibration. *J Sound Vib* 1998;215(4):841–62.
- [21] Arslan YZ. Experimental assessment of lumped parameter human body models exposed to whole body vibration. *J Mech Med Biol* 2015;15(1):1–13.
- [22] Deb K, Pratap A, Agarwal S, Meyarivan T. A fast and elitist multiobjective genetic algorithm: NSGA-II. *IEEE Trans Evol Comput* 2002;6(2):182–97.
- [23] Raquel C, Naval P Jr. An effective use of crowding distance in multiobjective particle swarm optimization. In: *Proceeding of GECCO'05, USA; 2005*. p. 257–64.
- [24] Holland JH. *Genetic algorithms*. Sci Am 1992:66–72.
- [25] Holland JH. *Adaptation in natural and artificial systems*. 1st ed. Michigan: MIT Press; 1975. p. 1–211.
- [26] Kusyk J, Sahin C, Uyar M, Urrea E, Gundry S. Self-organization of nodes in mobile ad hoc networks using evolutionary games and genetic algorithms. *J Adv Res* 2011;2(3):253–64.
- [27] Song L. *NGPM-A NSGA-II program in matlab – user manual*. Version 2011;4(1):1–20.
- [28] Song L. *NGPM-A NSGA-II program in matlab v14*. matlab code [cited 2015 March 15]. Available from <<http://www.mathworks.com/matlabcentral/fileexchange>> .
- [29] Kennedy J, Eberhart RC. Particle swarm optimization. In *proceedings of IEEE international conference on neural networks* 1995;4:1942–8.
- [30] Coello Coello CA, Pulido GT, Lechuga MS. Handling multiple objectives with particle swarm optimization. *IEEE Trans Evol Comput* 2004;8(3):256–79.
- [31] Smith A, Coit D. *Handbook of evolutionary computation*. 1st ed. Bristol (UK): Institute of Physics Publishing and Oxford University Press; 1997, C5.2: 1–11.
- [32] ISO: 2631-1. *Mechanical vibration and shock – evaluation of human exposure to whole-body vibration*; 1997.
- [33] Van Niekerk JL, Pielemeier WJ, Greenberg JA. The use of seat effective amplitude transmissibility (SEAT) values to predict dynamic seat comfort. *J Sound Vib* 2003;260:867–88.
- [34] Bovenzi M. Health effects of mechanical vibrations. *G Ital Med Lav Erg* 2005;27(1):58–64.
- [35] Wan Y, Schimmels JM. Optimal seat suspension design based on minimum simulated subjective response. *J Biomech Eng* 1997;119:409–16.
- [36] Zhang Y, Chen W, Chen L, Shangguan W. Non-stationary random vibration analysis of vehicle with fractional damping. In: *Proceedings of 13th National Conference on Mechanisms and Machines (NaCoMM07)*. p. 171–8.
- [37] ISO 8608. *Mechanical vibration – road surface profile – reporting of measured data*, 1st ed.; 1995.
- [38] Rosenthal S, Borschbach M. Impact of population size and selection within a customized NSGA-II for biochemical optimization assessed on the basis of the average cuboid volume indicator. In: *Proceedings of sixth international conference on bioinformatics, biocomputational systems and biotechnologies. BIOTECHNO*; 2014. p. 1–7.
- [39] Hernandez-Diaz AG, Coello Coello CA, Perez F, Caballero R, Molina J, Santana-Quintero LV. Seeding the initial population of a multi-objective evolutionary algorithm using gradient-based information. In: *Proceedings of IEEE congress on evolutionary computation 2008 (IEEE world congress on computational intelligence)*. p. 1617–24.
- [40] Reeves C, Rowe J. *Genetic algorithms – principles and perspectives A guide to GA theory*. 1st ed. Dordrecht: Kluwer Academic Publishers; 2003. p. 55–76.
- [41] Alander J. On optimal population size of genetic algorithms. In: *Proceeding of CompEuro'92 'computer systems and software engineering*. p. 65–70.